Journal of Experimental Botany, Vol. 46, No. 282, pp. 83–94, January 1995

Journal of Experimental Botany

Dynamic measurements of root hydraulic conductance using a high-pressure flowmeter in the laboratory and field

Melvin T. Tyree[1,2,3], Sandra Patiño[2], John Bennink[1] and John Alexander[1]

[1] *Aiken Forestry Science Laboratory, PO Box 968, Burlington, VT 05402, USA*

[2] *Smithsonian Tropical Research Institute, PO Box 2072, Balboa, Republic of Panama*

Received 9 May 1994; Accepted 5 October 1994

Abstract

A new high-pressure flowmeter (HPFM) is described which is capable of rapid water-flow measurements. The HPFM permits dynamic determination of hydraulic conductance of roots, K_r, and can be used in the laboratory or field. The base of a root is connected to the HPFM and water is perfused into the root system opposite to the normal direction of flow during transpiration. The perfusion pressure is changed at a constant rate of 3–7 kPa s^{-1} while measuring the flow into the root every 2–4 s. The slope of the plot of flow versus applied pressure is K_r.

This paper describes the HPFM, presents the theory of dynamic flow measurements, discusses sources of error, presents evidence that dynamic measurements of K_r in *Ficus maclellandi* (and six other tropical species from Panama) yield the correct result, and demonstrates the use of the method under field conditions in Panama on *Cecropia obtusifolia* and *Palicourea guianensis*.

Key words: High-pressure flowmeter, root and shoot hydraulic conductance, *Ficus maclellandi*, *Cecropia obtusifolia*, *Palicourea guianensis*.

Introduction

Recently Tyree *et al.* (1994) reported novel methods of measuring the hydraulic conductance of large woody root systems. Shoots were excised under water a few cm above the soil level, and the rootstock was fitted with water-filled tubing. Water was perfused into the base of the root system at a pressure P (MPa) causing water flow, F ($kg\ s^{-1}$), opposite to the normal direction of water flow during transpiration. A plot of F versus P was used to estimate root conductance, K_r, from the slope. Two types of measurements were performed. (1) Quasi-steady-state measurements in which P was held constant for 1–3 h until approximately constant F was observed. (2) Dynamic measurements in which P was changed every 3 min and F measured at the end of each 3 min interval even though F was still changing with time. The former method yielded approximately linear relationships between F and P with minor hysteresis; the latter method produced more hysteresis. Both methods produced slopes that were deemed to underestimate K_r.

Tyree *et al.* (1994) presented a model of the dynamics of solute and water flow in roots (AMAIZED) to interpret the results. AMAIZED predicted the observed hysteresis during dynamic measurements and predicted the underlying cause of the hysteresis. AMAIZED predicted that the driving force on water flow was constantly changing during the measurements. As solution was perfused down the root system, water was forced out of the roots and some solutes were retained by reverse osmosis. The retention of solutes caused a decline in solute potential inside the xylem of the minor roots during the measurement. The more negative solute potential reduced the water potential difference between the vessels and the soil which reduced the rate of water efflux across the radial pathway (=a non-vascular leaky osmotic barrier). The model predicted that both methods should underestimate K_r, but AMAIZED predicted that if the relationship between F and P could be measured more quickly then negligible changes in driving force would occur and approximately the correct conductance ought to be measured.

The purposes of this paper are to: (1) present the

[3] To whom correspondence should be addressed in USA. Fax: +1 802 899 5007.

design of a fast-response high-pressure flowmeter (HPFM) capable of rapid measurement of K_r; (2) present the theory of dynamic flow measurements and discuss the major sources of error; (3) present evidence that dynamic measurements of K_r yield the correct result; and (4) demonstrate the use of the HPFM for measurement of shoot and root conductances in the field.

Materials and methods

Plant material

Laboratory experiments were done on *Ficus maclellandi* King trees obtained from a commercial grower. This work was done in the fall of 1993 and *F. maclellandi* was chosen primarily because potted plants could be obtained in quantity and were of relatively uniform size. The trees were approximately 1.5 m tall, 20–30 mm diameter measured 20 cm from the base, had leaf areas of 0.5–1.2 m^2, and were 18–24-months-old. They were grown in 0.25 m diameter pots containing 10–12 L of soil which consisted of a 1 : 1 mix of topsoil and peat moss.

Field measurements were conducted in Panama on the Gigante peninsula (Barro Colorado National Monument, Smithsonian Tropical Research Institute, Panama) in March 1994. The region can be classified as a lowland moist forest having a rainfall of 2400 mm in the wet season (April through December) and 215 mm in the dry season (January through March). Species selected were *Cecropia obtusifolia* (Moraceae) and *Palicourea guianensis* (Rubiaceae). *C. obtusifolia* is a rapidly growing early gap colonizer tree. This species occurs from Mexico to Panama to Ecuador and grows 5–10 m tall with a sparse canopy. *P. guianensis* is a shrub or small tree to about 3.5 m tall, frequent at the edges of clearings and along the lake shore, and occurs from Guatemala to much of South America.

In July of 1994 additional laboratory experiments were conducted on seedlings of several tropical species growing in 0.12 m diameter pots. The species studied were: *Psychotria furcata*, *Psychotria marginata*, *Piper cordulatum*, *Piper culebranum*, and *Anacardium excelsum*. These plants had basal diameters of 3–5 mm, 0.02–0.08 m^2 leaf area and were from 3–6-months-old. An additional experiment was performed on an aerial root of a hemi-epiphyte (*Clusia uvitana*). The root had grown from an individual plant near a lake and the root had branched prolifically and grown to a length of 2 m in the water; it had a basal diameter of 5 mm at the point of excision from the plant.

High-pressure flowmeter (HPFM)

The HPFM is shown diagrammatically in Fig. 1. It is an apparatus designed to perfuse water into the base of a root system while rapidly changing the delivery pressure and simultaneously measuring flow.

The rapid change in water pressure was achieved using a pressure regulator (PR), a needle valve (NV), and a captive air tank (CAT). A pressure regulator (PR) delivered compressed air at a pressure of 4–5 MPa through a needle valve (NV). The NV was connected to the air-chamber (A) of a captive air tank (CAT). A rubber diaphragm separated the air from water (W) in the CAT. The NV was adjusted to permit a rate of air flow to pressurize the air volume at a rate of 3–7 kPa s^{-1}. The

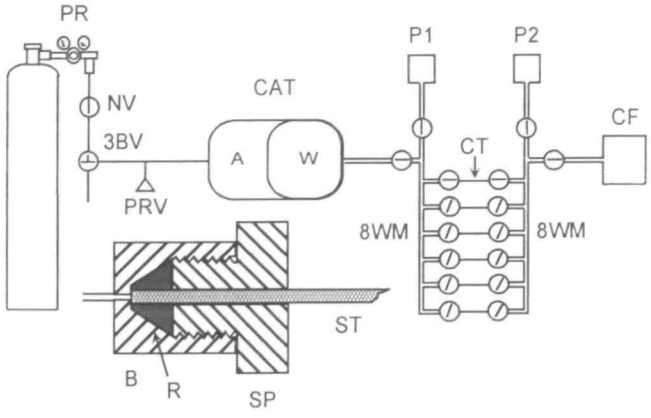

Fig. 1. Diagrammatic representation of the high-pressure flowmeter (HPFM) for rapid measurements of transient flow of water into root or shoots while rapidly increasing the applied pressure. Abbreviations are: 3BV, 3-way ball valve; 8WM, 8-way manifold; A, air space in CAT; CAT, captive air tank; CF, compression fitting to connect HPFM to root or shoot; CT, capillary tubes; NV, needle valve; P1, P2, pressure transducers one and two, respectively; PR, pressure regulator; PRV, pressure release valve; W, water-filled space in CAT. The compression fitting is shown in cross-section in more detail below the CAT. Abbreviations here are: B, base made of clear plastic; R, rubber stopper; SP, screw-driven plunger; ST, stem. When SP is screwed into B the stopper is compressed to form a watertight seal.

volumes of air and water were approximately equal in the CAT. The CAT could be pressurized or depressurized by turning the 3-way ball valve (3BV). It is best to use a CAT with approximately 2 L volume in A and W in order to use less gas for pressurization, but tanks up to 10 L volume have been used. A pressure release valve (PRV) prevented accidental over-pressurization. Since the pressure in A never exceeded 0.6 MPa, the pressure drop across the NV was approximately constant and thus the rate of pressurization was approximately linear with time.

Pressurized water was delivered from the CAT to an 8-way manifold (8WM) by way of 6 mm ID nylon-reinforced Tygon tubing. At a distance of 0.3 m from the input side of the 8WM the diameter of the tubing was reduced to 3 mm OD, 1.5 mm ID plastic tubing terminated with Swagelock[4] adapters; the plastic tubing was medical grade IV-tubing with LUER-LOK fittings capable of holding pressures up to 3.5 MPa. The 8WM is shown diagrammatically in Fig. 1; it was an Omnifit, 8-way, HPLC valve (Cat. No. 45-1103, Rainin Instrument Co., Woburn, MA) of octagonal geometry with 8-tubes emerging from a common point in the centre and each tube terminated by a valve.

On the inlet side, the 3 mm OD tube from the CAT was connected to one of the 8 valves and a pressure transducer (P1) was connected to another valve. On the outlet side another pressure transducer (P2) was connected to a second 8WM as well as the 3 mm OD outlet pipe. This left 6 pairs of valves available between each 8WM for connection of narrow-bore capillary tubes (CT). The capillary tubes were 1.5 mm OD HPLC tubing 0.16 m long, having internal diameters from 0.12–0.5 mm. During a measurement, one CT was selected by opening the inlet and outlet valves of the CT and closing the valves for all the other capillary tubes. Water flow across the

[4] The use of trade, firm, or corporation names in this publication is for the information and convenience of the reader. Such use does not constitute an official endorsement or approval by the US Department of Agriculture, Forest Service, of any product or service to the exclusion of others that may be suitable.

selected CT caused a pressure drop ($\Delta P = P_1 - P_2$) measured with P1 and P2, respectively. Calibration curves were established relating flow, F, to ΔP values in the range of 0–100 kPa. Capillary tubes up to 0.25 mm ID had linear calibration curves, whereas tubes 0.3 mm ID or larger were non-linear because of the transition from laminar to turbulent flow.

The pressure transducers used were model C204 (Setra Inc. Acton, MA) having a range of 0.4 MPa and a resolution of ±0.1 kPa. Transducers with a range of 0.7 MPa were used later in order to improve the accuracy of the measurements for reasons stated below. Less expensive transducers (model PX136-100GV, Omega Engineering Inc., Stamford, CT) were also used and performed nearly as well although they required calibration against a model C204 transducer. The output of the pressure transducers were logged using model D11×1 series modular data-loggers depending on the voltage range needed (Omega Engineering).

The outlet side of the 8WM was connected by a 0.3 m length of water-filled 3 mm OD (1.5 mm ID) tubing to a compression fitting (CF) that permitted connection to a plant or root base. The CF is as described in Tyree (1983) and is shown in cross-section in more detail in Fig. 1.

For experiments on seedlings done in July 1994, we had to increase the sensitivity of the HPFM to measure smaller F values. This was achieved by employing a CT with an ID of 0.12 mm and length of 1.5 m. The full scale range of F was 0 to 2×10^{-7} kg s^{-1}. To measure small flows we had to take more care to exclude air bubbles from the HPFM and we had to reduce the elasticity of the tubing on the outlet side of the HPFM by replacing the IV-tubing with more rigid plastic HPLC tubing 1.5 mm OD and 1 mm ID. A smaller CF was fabricated to connect to the seedlings. The HPFM may be available soon from Dynamax Inc., Houston, Texas.

Transient root conductance measurements

The pots of *Ficus* were submerged in a water bath and shoots were excised under water about 0.2 m above the soil to leave enough stem for later manipulations. The HPFM was connected to the root system via the CF. Three to five transient flow measurements were made immediately. During each transient P_1 was increased at the rate of 3–7 kPa s^{-1} while measuring instantaneous F once every 2–4 s. After a brief lag, P_2 also began to increase linearly with time at a slightly reduced rate because of the pressure drop across CT. The entire sequence of measurements took 80–150 s to complete. A CT was selected by trial and error to have a conductance approximately 5 to 20 times that of the root system so that the ΔP was within the calibration range for accurate determination of F. The F was plotted versus the applied pressure driving flow into the root, P_2, using SigmaPlot (Jandel Scientific, San Rafael, CA). The curves were non-linear for the first 0.05–0.2 MPa followed by a distinctly linear region for higher values of P_2 (see results). Transient root conductance, K_{rt}, was computed from the slope of the linear region by linear regression of the data.

After the initial transient measurements of K_{rt}, the HPFM was removed from the root system and the entire pot was placed inside a root-pressure chamber for quasi-steady-state determination of root conductance, K_{rq}, see below. Following the determination of K_{rq}, 3 to 5 more transient measurements of K_{rt} were made.

Quasi-steady-state measurements

A large pressure chamber was constructed from the steel pipe used in steam-heating plants. The pipe was 0.45 m ID and 1.2 m long and was terminated by a 35 mm-thick metal cap and rubber seal that mated with the pipe. The pot with root and soil was placed in the chamber and the 0.2-m-long stem base protruded through another rubber seal to the outside air. The pressure chamber was pressurized with an air compressor. The compressed air forced water to move from the soil mass into the root system and out of the base of the stem segment via the xylem. A peristaltic pump was used to pump water from the stump to a container on a digital balance. A computer connected to the digital balance computed F from the root system by measuring the weight of water in the container at 5 min intervals.

The pressure in the chamber was adjusted up or down once every 30–60 min and a plot of F versus applied pressure was constructed from 4 to 8 points and values of K_{rq} were computed from linear regression lines. Flows changed slowly because of gradual changes in soil-water-content or root properties. So the measurements were quasi-steady-state. But similar methods have been used in the past to estimate K_{rq} of roots in soil (Saliendra and Meinzer, 1992; Levy *et al.*, 1983) or immersed in a liquid media (Ramos and Kaufmann, 1979; Salim and Pitman, 1984; Markhart and Smit, 1990).

Pressure chamber measurements on seedlings in July were performed in a similar way except that the chamber was smaller. The stems of seedlings were excised 10–20 mm above the soil and were not long enough to pass through the rubber seal in the lid of the pressure chamber. The potted plants were placed in the bottom of the chamber and a 1 m length of HPLC tubing 0.3 mm ID was fitted to the rootstock via a small CF. The HPLC tube passed through the rubber seal on the lid of the pressure chamber and delivered water to the electronic balance.

Transient measurements on a physical model of roots

During steady-state measurements of water flow in roots, all the water that flows into a root must, by definition, flow out. But some water can accumulate in the roots during transient measurements. If roots were initially dehydrated some water entering the roots would rehydrate the living cells and remain in the root.

The rate of water flow into roots, F, will exceed the rate of passage through the roots, F_h, even in fully-hydrated roots because pressurization will cause elastic swelling of roots and compression of any air-bubbles that might be present in the wood. So F will be given by:

$$F = F_h + F_e + F_b \qquad \text{(A1)}$$

where F_e is the flow associated with elastic swelling and F_b is the flow to compress air bubbles (when present). The theory behind Equation (1) is given in Appendix 2.

A linear rate of pressure increase was chosen because in theory that would make F_e a constant. Also F was measured to pressures of 0.35–0.5 MPa because the flow for bubble compression, F_b, falls rapidly with increasing pressure.

Physical models of root systems were constructed in order to study the effect of elasticity and bubble compression on the determination of conductance from transient measurements. The physical model consisted of six, 60 mm lengths of rigid 0.12 mm ID capillary tubing connected in series through T-tubes with valves at each arm of the T. The six lengths of rigid tube in series had about the same conductance as the *Ficus* roots. The T-tube connector permitted the installation of elastic side-tubes of 1.5 mm ID tubing. The side-tubes could be filled with water or a combination of water and air. When the side-tubes were closed off, measurements of transient conductance could be made with minimal elasticity. When the side-tubes were opened, transients could be measured with controlled amounts of elasticity and air-bubbles present.

Other measurements were done to determine the temperature dependence of the calibration factor (=the slope of the plot of F versus ΔP) in the HPFM. The entire apparatus was placed inside a constant temperature box and the calibration was measured at 5 °C intervals from 5–35 °C. The calibration factor, K_{CT}, should be a function of viscosity, η, of the water passing through the CT and a function of the temperature dependence of the electronics (pressure transducers, voltage regulator and data loggers). The viscosity contribution to the K_{CT} for each CT should be given by the Hagen-Poiseuille equation, i.e. $K_{CT} = \pi r^4/8\eta L$, where r is the internal radius of the CT, L is the CT length, and η is the viscosity of water which changes about 2% per °C.

Field measurements

Work in Panama was undertaken primarily to see how well the HPFM performed under field conditions. Two limited objectives were sought: (1) to examine how root and shoot conductances increase as plants grow and (2) to relate root conductance to measures of root size.

P. guianensis was available in a range of sizes from four mature leaves and 4 mm basal stem diameter to larger plants with 40–50 leaves and 16 mm basal diameter. The objective was to determine how root and shoot hydraulic conductances increased with plant size. Our measure of plant size was leaf area measured with a LiCor 3100 leaf area meter. Whole shoot conductances with leaves present and after removal of leaves were measured with the HPFM as described in detail in Yang and Tyree (1994). Briefly, shoots were excised from roots under water by constructing a watertight container around the base of each plant. The HPFM was connected first to the root and conductance measured by 2 to 3 transients as described above. Then the HPFM was connected to the base of the shoots and the pressure (P_2) was set at 0.5–0.55 MPa which caused rapid perfusion of the shoots. After 10–15 min leaf air spaces filled with water which began dripping from the stomates; this corresponded to a time when shoot conductance became relatively stable (quasi-steady-state). After recording the whole shoot conductance ($K_s = F/P_2$), the leaves were excised causing an increase in conductance which was also recorded.

Soil was removed from the base of 4–8 m tall *C. obtusifolia* trees to expose a range of woody roots from 3–15 mm basal diameter of wood. The roots were excised under water and connected to the HPFM and the K_{rt} measured with 2 to 3 transients as described above. The hypothesis was that K_{rt} ought to increase approximately with basal diameter (or wood cross-section). When only a weak correlation was found (see results), the roots were removed from the soil to estimate their surface areas to see if a better correlation could be found. Roots were removed hydraulically, which was done most conveniently on plants growing on slopes. A gasoline water pump was used to deliver water via a fire-hose to a nozzle. The jet of water controlled by the nozzle was used to wash the soil away from the roots. This method recovered fine roots < 1 mm diameter although many were broken. Roots were returned to the laboratory and projected area was estimated on roots < 6 mm diameter by running them through the leaf area meter. Total surface area (recovered) was estimated by multiplying the projected area by π (assuming cylindrical geometry).

Results and discussion

Laboratory measurements

Temperature dependence of the HPFM: The temperature dependence of the calibration factor, K_{CT}, is given in Fig. 2. Values of K_{CT} are shown normalized to the value at 20 °C (Fig. 2A). The slope revealed a temperature dependence of 2.25% of the normalized value per °C which was close the temperature dependence of the normalized value of inverse viscosity. The temperature dependence of K_{CT} should be given by,

$$K_{CT} = (\pi r^4/8\eta L)\, K_e \qquad (1)$$

where K_e is the temperature dependence of the electronics. Thus a plot of $K_{CT}\eta$ should equal $K_e \pi r^4/8L$. The plot of $K_{CT}\eta$ versus temperature is shown in Fig. 2B. The temperature dependence of the electronics was approximately −0.18% of the normalized value per °C.

These data suggest that the HPFM should be calibrated at a known temperature; when measurements are made at different temperatures, values of F (and thus root or

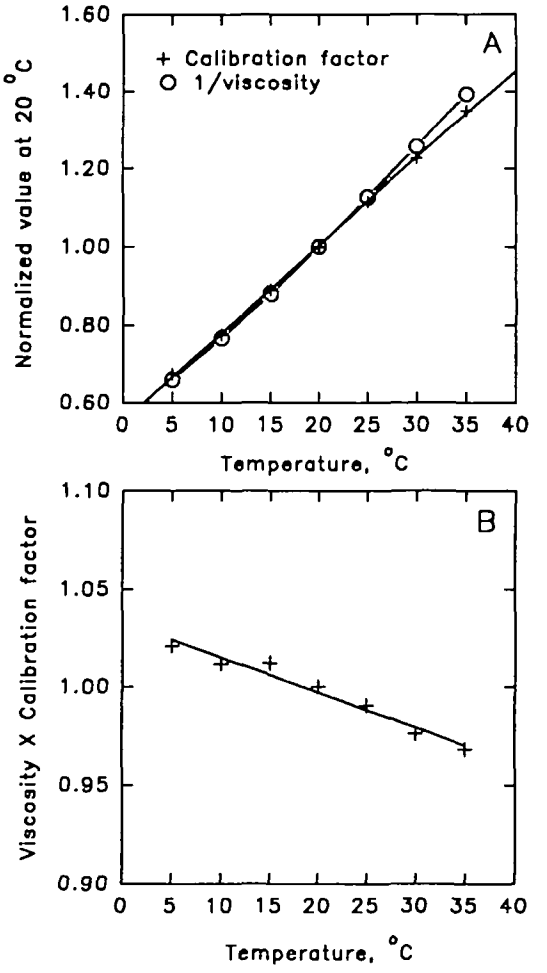

Fig. 2. The temperature dependence of the HPFM. Each CT has a calibration factor (K_{CT}) that relates flow to the pressure drop across the CT, i.e. $F = K_{CT}\Delta P$. (A) The x-axis is the temperature at which the K_{CT} was measured and the y-axis is the normalized value of K_{CT} and of the inverse viscosity of water, i.e. the value at temperature T divided by the value at 20 °C. (B) The normalized value of the remaining temperature dependence of the HPFM after elimination of viscosity effects. The slopes of the straight lines are 0.0225 and $-0.0018\ °C^{-1}$ in (A) and (B), respectively.

shoot conductance) should be corrected by 2.25% °C^{-1}. The correction is nearly equal to that due to changes of the viscosity of water flowing through the HPFM. In practice, it is unlikely that the temperature of the HPFM will always equal the air temperature, especially under field conditions when the HPFM may be in the sun or the shade at different times. But if the temperature of the HPFM is known within, say, ±3 °C then the values of F and conductance can be taken to be accurate to about ±7%. It should be remembered that the conductance of the objects being measured will be temperature dependent too. So conductance measurements should be reported together with the temperature range at which measurements were performed.

Physical model of a root

Transient measurements of F versus P_2 were measured on a physical model of a root consisting of six rigid segments of capillary tube connected in series with elastic side-arms between each rigid segment. The tubing of the side-arms simulated the bulk modulus of elasticity of real roots. P_2 was increased at the rate of 3.3 kPa s^{-1} while measuring F every 4 s. When the side-arms were closed off to simulate low elasticity, F versus P_2 was a linear function over the entire range of the data (Fig. 3A, dots). When side-arms were opened, F versus P_2 was curved for the first 0.1 MPa then approached a linear relationship with a slightly higher slope than before (compare dots to triangles in Fig. 3A). The length of the rigid tubes and of the side-arms were selected by trial and error to yield transient curves similar to those in *Ficus* roots (see below).

The HPFM was designed to provide an approximately linear rate of increase of P_2 because, in theory, flow to cause elastic swelling ought to be independent of time. The effect of elastic flow is to displace the linear part of the curve upward in the graph of F versus P_2 without changing the slope. The theory is developed in detail in Appendix 2. The side-tubes had a measurable plasticity, i.e. when the pressure was held constant at the end of a transient, water continued to flow into the side-tube at a decreasing rate over the next few minutes (data not shown). The plasticity of the side-tubes accounted for the change in slope seen in Fig. 3A. If roots also exhibit a combination of elastic and plastic stretch under pressure, then the slope of a transient might cause an overestimate in K_r.

Occasionally an air-bubble was inadvertently trapped in the CF between the HPFM and the real- or model-root. When this happened a differently shaped transient was observed as shown in Fig. 3B. Shown are transient curves for 0.0, 0.1 and 0.5 ml of air into the side-arm nearest the HPFM. A bubble of 0.1 ml caused a transient plateau and a 0.5 ml bubble caused a distinct peak at $P_2 = 0.06$ MPa. In all cases the plots of F versus P_2 tended

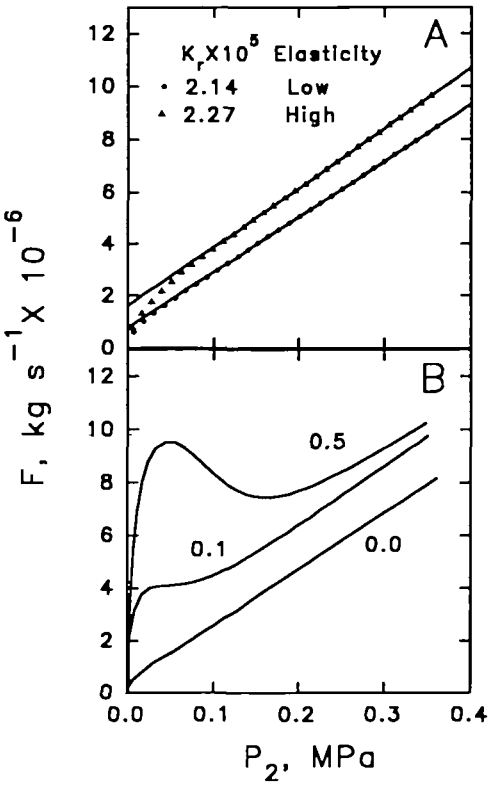

Fig. 3. Transient measurements of water flow rate (F) versus applied pressure (P_2) in a physical model of a root system. The model consisted of six lengths of capillary tube in series having a steady-state conductance (K_r) similar to that of *Ficus* roots. (A) Effect of elasticity on the shape of the transient curves. High and low elasticity was obtained by including or excluding elastic side-tubes in the physical model. Slopes = dynamic K_r values are given in the figure. (B) The effect of air bubbles between the HPFM and the model root. The numbers next to the curves are the bubble volumes in ml.

to approach the same limiting slope after the initial transient.

Transients of the form of the 0.1 ml curve were occasionally observed in *Ficus* experiments. Curves of the form of the 0.5 ml curve were occasionally observed in field experiments in Panama. In theory (Appendix 2) the rate of flow to cause bubble compression is given by

$$F_b = [V_i P_i/(P_2+0.1)^2]dP_2/dt. \qquad (A7)$$

Equation (A7) was derived from the ideal gas law where V_i and P_i are the initial volume and pressure of the bubble, respectively. This equation applies to a bubble trapped between the root and the HPFM where P_2 is measured, but the same equation applies at any location where a bubble might be present where P_2 is taken as the fluid pressure adjacent to the bubble. Equation (A7) shows that the rate of flow to compress bubbles is proportional to the rate of change of P_2, which is a constant in our experiments, and inversely proportional to the square of the absolute pressure $= (P_2+0.1)$. The value of F_b fell rapidly with increasing P_2 (see Appendix

2), so the HPFM was redesigned after the *Ficus* experiments to permit pressure increases up to 0.6 MPa in order to improve the accuracy with which the final slopes ($=K_{rt}$) could be determined.

The physical model of the root was also used to investigate the effect of having air-bubbles distributed evenly along the 'root' resistance. Figure 4 shows the effect of having an 0.05 ml bubble in the second through sixth side-arms downstream from the HPFM, so a total of 0.25 ml of air was evenly distributed along the 'root' resistance. When P_2 was increased at the rate of 3.33 kPa s^{-1} an exaggerated initial transient was observed followed by a slope that underestimated the K_r of the model root. This shape of curve occurred because most of the flow into the model root was going to compress the bubbles. Curves of this shape were never observed in experiments on real roots, thus when air bubbles were present in real roots, they were located between the HPFM and the main resistance to water flow in the root.

When P_2 was increased more slowly with time (Fig. 4), the flow through the system approached a quasi-steady-state. So the flow to compress bubbles became a smaller fraction of the total flow through the system, and the slope in the pressure range of 0.2–0.35 MPa more nearly approached the correct value.

Ficus *roots*

Figure 5 shows typical measurements of water flow from roots pressurized in a root chamber. Steady-state flow was never reached. Figure 5A shows F versus time when a *Ficus* root was pressurized at a constant applied pressure of 0.5 MPa. During this experiment a total of 2.5 L of water was extracted from a soil mass of 10 L volume. Thus the soil water potential was constantly changing. Also the elevated gas pressure on the soil mass may have caused a progressive change in root conductance.

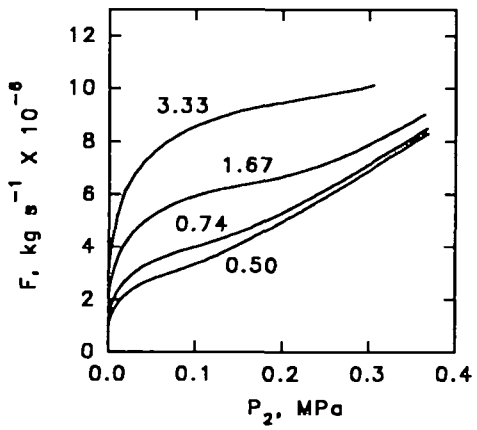

Fig. 4. Transient measurements of water flow similar to Fig. 3, but with air-bubbles distributed in the five side-arms between the six lengths of capillary tube. Each side-arm contained 0.05 ml of air. The numbers next to the curves are the rate of increase of P_2 in kPa s^{-1}.

Figure 5B shows another experiment in which the applied pressure was held initially at 0.6 MPa for 1 h then adjusted every 0.5 h through the following pressure sequence: 0.4, 0.2, 0.1, 0.25, 0.45, and 0.65 MPa. The flow at the end of each pressurization period versus the applied pressure is shown in Fig. 5C. Stable flows were never reached; consequently, all measurements in Fig. 5 must be viewed as quasi-steady-state. The K_{rq} values were calculated from the regression line of the data set. Since the root and/or soil properties changed during the measurement, we measured transient conductances before and after the quasi-steady-state measurements and used the mean of the values before and after to compare to K_{rq}.

The quasi-steady state measurements of F of root systems in a pressure chamber, must be rate-limited by a combination of soil and root resistance to water flow. It is generally assumed that wet soils contribute little to the soil–root resistance (Newman, 1969; Caldwell, 1976). Flow should decrease constantly when a constant pressure is applied to the soil mass because as the soil-water-

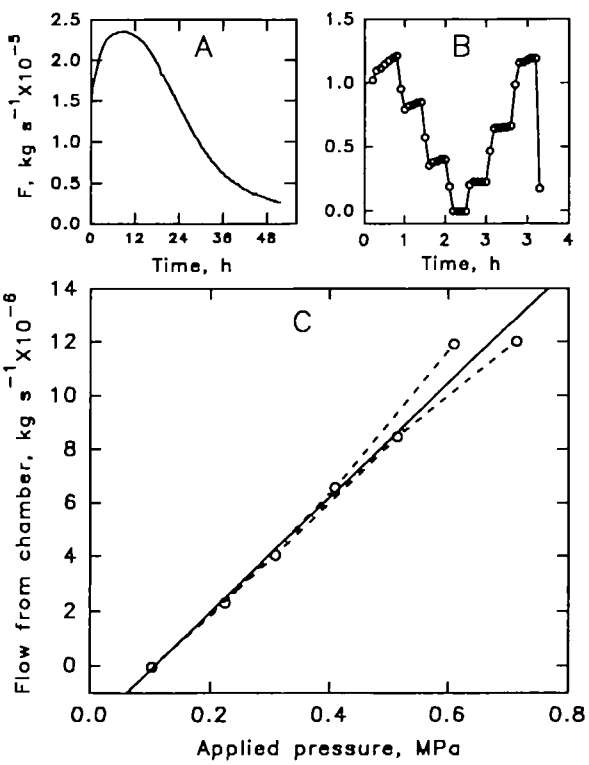

Fig. 5. Quasi-steady-state measurements of flow (F) for a *Ficus* root system in a pot enclosed in a pressure chamber. The chamber was pressurized with compressed air to drive water from the soil mass through the root and out of the stem that protruded through a rubber seal to the outside air. All measurements were made at 20–26 °C. (A) Flow versus time with a constant applied pressure of 0.5 MPa starting with soil saturated with water. (B) Flow versus time while changing the pressure from 0.5 MPa to 0 in three steps then from 0 to 0.55 MPa in three steps. (C) Flow versus applied pressure at the end of each pressure step for the experiment shown in (B). Dashed line connects the points in the sequence of measurement and the solid line is the linear regression of the points $=K_{rq}$ (the quasi-steady-state root conductance).

content declines the water potential of the soil (ψ_{soil}) should decline reducing the flow.

The puzzling initial rise in flow during the first few hours of the experiment (Fig. 5A, B) suggests either an increase in driving force or an increase in conductance of the root. An increase in driving force could result if the solute potential in the xylem of minor roots declined during the first few hours. Solute accumulation (which would lower solute potential) was unlikely, because the concentration of all major cations in the exudate declined during the first few hours (data not shown). The increase in F occurred whether the roots were pressurized with air or nitrogen, so a possible role of increased oxygen concentration which might affect respiration was eliminated. Until more work is done, we can say only that roots were being altered during the quasi-steady-state measurements.

A typical transient curve of F versus P_2 is shown in Fig. 6A. The rate of pressure increase was 3.3 kPa s^{-1} and flow readings were taken at 4 s intervals. The curve was typical of many observed for *Ficus* roots; the data were similar to that shown in Fig. 3A (triangles) and was indicative of a transient caused by elasticity (see Appendix 2). A comparison of K_{rt} to K_{rq} for nine *Ficus* root systems is shown in Fig. 6B together with data comparing K_{rt} to K_{rq} measured on one seedling of each of six other species. The principal factor determining root conductance was the size of the root system, thus the conductances of the seedlings were about one order of magnitude less than the conductance of the larger *Ficus* roots. The regression line did not deviate significantly from the 1 : 1 line indicating equality between K_{rt} and K_{rq}. (A log–log plot was used in Fig. 6 and elsewhere because (1) regressions on log–log plots can reveal linear and well as non-linear correlations and (2) log scales permit a better display of data ranging over more than one order of magnitude.) These data support the hypothesis that both methods measured the same quantity. Although the conductances are reported as 'root' values, the values must include some soil limitation to water flow. How much of the conductance was due to soil and how much was due to root is unclear. The soil was initially saturated with water because the root systems were immersed in water prior to cutting under water. In water-saturated soils the resistance to water flow is likely to be less than in the root.

The purpose of the studies on *Ficus* roots and on the seedlings was to compare root conductances measured by independent methods, i.e. transient conductance measurements, K_{rt}, measured with the HPFM and quasi-steady-state measurements, K_{rq}, measured with potted roots in a pressure chamber. The two methods had different sources of error.

Flow was induced in the normal direction of transpiration when a root system was pressurized in a pressure chamber. The advantage of this method was that the solutes that were taken up by the root were constantly

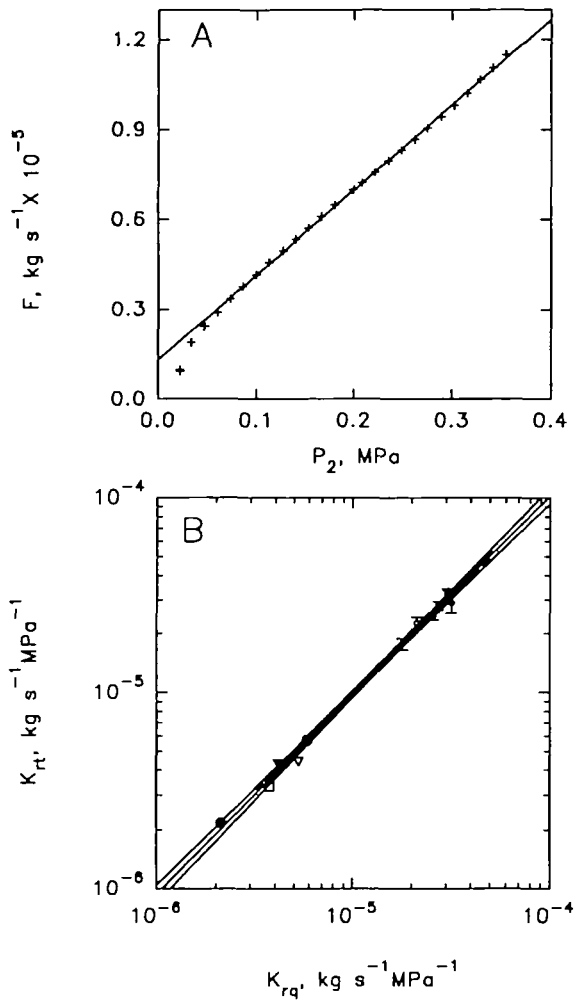

Fig. 6. (A) A typical dynamic response curve for a *Ficus* root. P_2 was increased at the rate of 3.3 kPa s^{-1} and flow measurements were recorded every 4 s (pluses). The slope of the solid line was used to compute K_{rt} (the transient root conductance). (B) Transient root conductance (K_{rt}) versus quasi-steady-state root conductance (K_{rq}) of nine *Ficus* roots (small circles) (●) *Clusia uvitana*; (▽) *Psychotria furcata*; (▼) *Psychotria marginata*; (□) *Piper cordulatum*; (■) *Piper culebranum*; (△) *Anacardium excelsum*. Two to three measurements of K_{rt} were made before and after the measurement of K_{rq}. Points are means ±SD of K_{rt} (N=4–6). Straight line is the regression of K_{rt} versus K_{rq} and curved lines are 95% confidence interval. All measurements were made at 20–26 °C.

swept out of the root system. As the applied pressure increased, the flow of water through the root increased and the internal solute concentration in the xylem of the root system approached zero. Consequently, the slope of flow versus applied pressure approached the true conductance.

The disadvantage of measuring root conductance with the HPFM was that the direction of flow was opposite to the normal direction of transpiration. The reversed flow into the root system caused the concentration of solutes by reverse osmosis. This lowered the solute potential in the xylem of the fine roots which caused a reduction in driving force and flow. The higher the applied pressure

the faster the solute accumulated by reverse osmosis. Tyree *et al.* (1994) demonstrated that a substantial change in solute potential occurred in minutes and this caused errors in the estimation of root conductance. Rapid measurement of F versus P_2 minimized the change in solute potential. But rapid measurements were subject to other errors because some flow during transient measurements was due to elastic swelling and bubble compression as discussed above and in Appendix 2; both these errors were absent during steady-state measurements in the pressure chamber. The observed agreement between K_{rt} and K_{rq} supports the hypothesis that the transient errors were negligible in *Ficus* and in the other six species.

Field measurements

Transient curves of F versus P_2 were of both forms in Fig. 3A (no air present) and 3B (0.1 ml bubble). Air was more frequently present in the roots in the field than in the laboratory experiments. Since the roots were cut under water and the CF connected while immersed, it was probable that the air was present prior to cutting. Measurements were done near the end of the dry season so the embolisms may have been caused by drought-induced-cavitation (Tyree and Ewers, 1991). In order to reduce errors in the measurement of K_{rt} caused by embolisms, the transient F was measured to higher P_2 values (up to 0.5 MPa).

A weak correlation was found between basal wood diameter of *C. obtusifolia* roots and K_{rt}; the slope of the trend in Fig. 7A was not significantly different from 0 at the 0.95 confidence level, but was significant at the 0.9 level. Basal diameter was a poor measure of root size because some roots tapered in diameter rapidly over a distance of 0.5 m without branching whereas others tapered gradually over several metres. There was a stronger positive correlation between K_{rt} and recoverable root surface area (Fig. 7B). The strong correlation with surface area was consistent with the hypothesis that the main resistance to water flow in large roots was in the non-vascular radial pathway rather than the axial vascular pathway (see Tyree *et al.*, 1994, and papers cited therein).

The hydraulic conductance of *Palicourea* roots and shoots were approximately equal, except in the smallest plants. K_s measured with leaves removed exceeded K_{rt} in all but one case (squares, Fig. 8A). K_s measured with leaves attached were generally about half the K_s measured with leaves removed (compare circles with squares at any given K_{rt} in Fig. 8A). This suggested that leaf resistance to water flow was approximately equal to the vascular resistance to water flow in stems.

K_s values increased with leaf area attached (closed circles, Fig. 8B) which was consistent with the need for higher conductance in shoots bearing more leaves. K_{rt} values followed a more curvilinear trend with leaf area

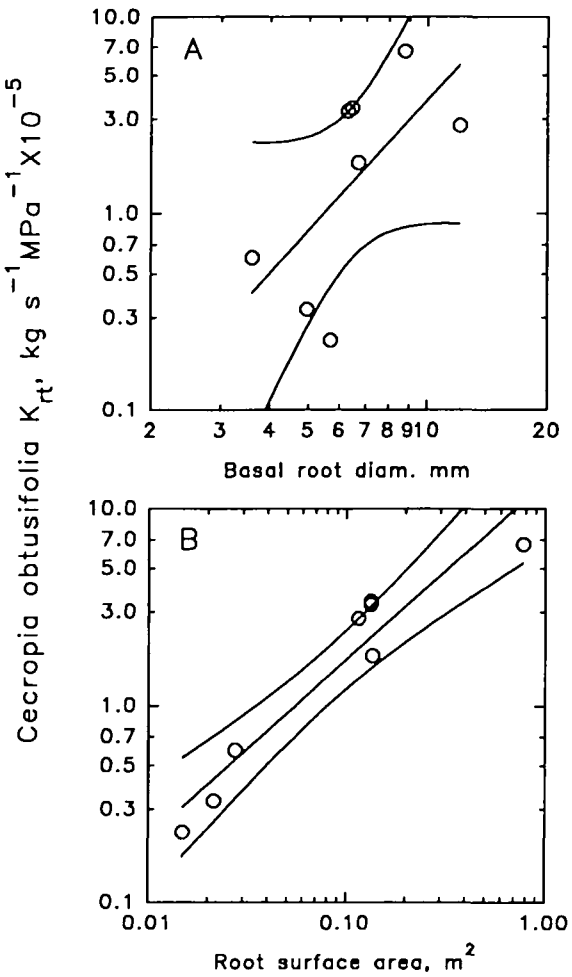

Fig. 7. Field measurements of transient conductance of *Cecropia* roots excised in the base of 5–8 m trees (temperature 25–31 °C). (A) K_{rt} versus basal diameter (wood) measured where excised. (B) K_{rt} versus recovered surface area of roots. Roots were recovered after measuring K_{rt} by using a fire-hose to wash soil away.

(open circles, Fig. 8B). In large plants the regression lines were not significantly different, but in the smallest plants K_{rt} was approximately twice K_s. The smallest plants were seedlings with just four leaves. The higher K_{rt} values of young seedlings suggested that small plants need to invest more in root growth than shoot growth to survive through the dry season.

Conclusions

The HPFM provides a rapid measurement of K_r. The method is similar in many respects to the pressure-probe method (Steudle, 1993). Both the pressure-probe and HPFM methods can be classified as rapid measurement methods, but the set-up time for the pressure-probe is generally much longer. In the pressure-probe method, an excised root is connected via a small, water-filled chamber to a pressure transducer. The chamber volume is held constant, and the root is left for 10–30 h while 'root-

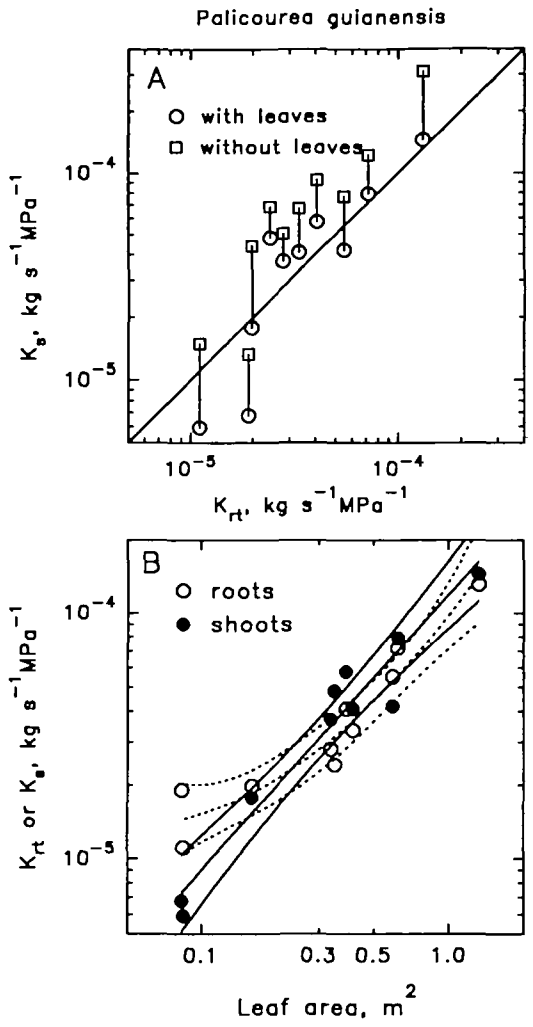

Fig. 8. Shoot and root conductances measured on small woody shrubs of various sizes (temperature 25–31 °C). (A) Shoot conductance (with and without leaves) versus root conductance. Vertical solid lines join shoot conductances measured on the same plant with and without leaves. Values are plotted versus root conductance. Diagonal line is the line for equality between root and shoot conductance. (B) Root and shoot conductance versus leaf area (as a measure of plant size). Middle solid line is the linear regression and curved solid lines are the 95% confidence intervals. The root data were fitted with a quadratic equation (middle dotted line) and the 95% confidence intervals on either side of the middle dotted line.

pressure' builds up due to solute accumulation in the root. This pressurization period is needed to dissolve air bubbles that interfere with subsequent measurements. The measurement of K_r is effected by rapidly changing the volume of the chamber (by moving a metal rod into or out of the chamber) and measuring how pressure changes with time. Measurement accuracy is strongly compromised by bubbles, because measurements are performed with relatively small volume and small pressure changes at pressures of about 0.05–0.2 MPa (in which flow for bubble compression is most). In contrast, measurements with the HPFM require a very short set-up time and were less affected by air bubbles. The disadvantages of the HPFM method in contrast to the pressure-probe method are: (1) small roots can not be measured with the HPFM as presently constructed and (2) the method can not be used to infer solute permeabilities and reflection coefficients.

The use of a HPFM for the measurement of root and shoot conductances is a novel approach to an old goal of measuring the component conductances in the soil–plant–atmosphere continuum. The advantages of the method are: (1) it is rapid. The time required to cut the plant, connect the HPFM and obtain a root conductance is 5–10 min. Since measurements are rapid, concerns about how shoot excision might affect root properties are minimized. (2) The HPFM can also be used to compare root-to-shoot conductances. An additional 15–30 min are required to measure shoot values. (3) Measurements are not restricted to potted plants (as in the pressure chamber method) and are not restricted to relatively small roots (as in the pressure-probe method, e.g. Melchior and Steudle, 1993).

The evidence that the HPFM measures K_r correctly must still be taken as tentative. The evidence is: (1) the observed relationship between F and P_2 is linear after an initial non-linear phase due to elasticity and bubble compression; (2) transient and quasi-steady-state conductance values agree in *Ficus* roots and in six other species and (3) the values of K_r change with measures of root and plant size as one might expect intuitively.

The HPFM may be of use to a wide range of research programmes of interest to agronomists, plant physiologists and ecologists. For example, we are currently using the method to study; (1) the seasonal progression of root and shoot conductance in *Acer* saplings; (2) the effect of soil temperature and water potential on root conductance; (3) the contribution of mycorrhizae to the enhancement of root conductance and (4) the contribution of root conductance, root biomass allocation, and root extension growth to seedling establishment of old-forest trees in Panama.

Finally, the HPFM may provide a means to study why some roots are leaky to backwards flow of water from roots to dry soil and others are not. For example, Nobel and Sanderson (1984) have shown that the hydraulic conductance of root systems of two desert succulents fell to very low values in dry soils. The decline in conductance was caused primarily by a reduction by many orders of magnitude in radial conductance and has been termed a 'rectifier-like activity'. But in arid-zone *Artemisia* roots there was substantial backward flow (Richards and Caldwell, 1989). At night a flow of water occurred from deep roots in moist soil to shallow roots in dry soil. The efflux of water from the shallow roots caused a localized rehydration of the soil—a process called 'hydraulic lift'. Hydraulic lift has been well documented in more mesic ecosystems (Dawson, 1993) where 'hydraulically-lifted

water' improved the water balance of upper soil layers and the water balance of shallow-rooted plants. Roots having substantial hydraulic lift are clearly more leaky to back-flow of water than roots of desert succulents.

In the strict electrical sense, a rectifier is a device with a high electrical conductance for current flow in one direction and a low conductance for current flow in the opposite direction. Rectification of water flow in roots should not be confused with an equal reduction of hydraulic conductance for both directions of flow as soil water potential declines. In a less-strict sense, rectification of water flow in roots may be caused either by an unequal radial conductance to water flow or by a change in driving force on water flow during back-flow not found during forward-flow.

A change in driving force can arise because of differences in what causes axial versus radial flow of water in roots. Axial water flow in vessels is caused solely by hydrostatic pressure differences and not by osmotic pressure differences because there is no osmotic barrier to solute flow along the axis of vessels. But for radial flow there is some osmotic barrier making the conductance of water more than the conductance of solutes. So, during back-flow, solutes and water travel together without selection down the axis of roots, but water passes radially out of roots with less selection than solutes. The consequence is an increase in solute concentration in the lumen of vessels in minor roots which reduces the driving force to the outward flow of water.

This process can be studied with the HPFM by causing a pressure-induced back-flow of solution with a constant applied pressure. F starts out high and then declines to a low but constant rate after several hours. The processes involved are described in detail by Tyree *et al.* (1994). Steady-state is reached when the rate of flow of solutes down the axis is balanced by radial leakage of solutes out of the fine roots. A root with a low radial solute permeability and high reflection coefficient would strongly rectify flow, i.e. the initial F after pressure is applied would be many times more than the steady-state F. Roots with low rectifying properties would have a high permeability to solutes and low reflection coefficient causing the initial and final flows to be more equal.

We think there may be big differences in solute-induced rectification between species, this was evident from how much transient values of K_{rt} declined following repeated measurements of root conductance. In some species K_{rt} did not decline significantly with repeated measurements, whereas in other species K_{rt} declined 10–30% between consecutive transients.

Appendix 1

Symbols and abbreviations used

$F=$ total flow through the flowmeter ($kg\ s^{-1}$)
$F_b=$ component of F causing bubble compression
$F_e=$ component of F causing elastic swelling of flowmeter and sample
$F_h=$ component of F passing through the system (usually root) being measured
HPFM= high-pressure flowmeter
$K=$ conductance ($kg\ s^{-1}\ MPa^{-1}$)
$K_r=$ 'true' root conductance
$K_{rt}=$ root conductance measured by transient method
$K_{rq}=$ root conductance measured by quasi-steady-state method in root pressure chamber.
$n=$ number of moles of gas in bubbles
P_1 and $P_2=$ pressures (MPa, relative to barometric pressure) in the inlet and outlet of the flowmeter, respectively
$P_b=$ absolute pressure of gas in a bubble
$P_i=$ initial absolute pressure of bubbles
$R=$ gas constant
$T=$ Kelvin temperature.
$V_b=$ volume (m^3) of bubble at pressure P_b
$V_i=$ initial volume of bubbles
$\Delta P=$ the pressure drop across a selected capillary tube in the HPFM
$\epsilon=$ bulk modulus of elasticity ($MPa\ m^{-3}$) of flowmeter and sample

Appendix 2

Theory of the dynamics of water-flow in a high-pressure flowmeter

A dynamic flow measurement is defined as a measurement of flow, F ($kg\ s^{-1}$), while pressure at the outlet of the flowmeter, P_2 (MPa), changes with time, t(s). In contrast, a steady-state flow measurement is defined as a measurement of F when P_2 is held constant. Under dynamic conditions there are three components of F, i.e. flow through the system being measured, F_h, flow associated with bulk elastic swelling of the system as the pressure increases, F_e, and flow to compress air bubbles that might be present in the system, F_b:

$$F=F_h+F_e+F_b. \tag{A1}$$

If the flow through the object measured is a linear function of applied pressure difference between the outlet of the HPFM and atmospheric pressure, we can express F_h as:

$$F_h=KP_2 \tag{A2}$$

where P_2 is the outlet pressure relative to atmospheric pressure. The volume of the tubing, connectors, and object measured will increase with P_2. If the volume increase is elastic and linear with pressure then the volume of the system, V, will be given by:

$$V=V_o+P_2/\epsilon \tag{A3}$$

where V_o is the initial volume of the system at $P_2=0$ and ϵ is the bulk modulus of elasticity. The time derivative of Equation (A3) gives the flow to cause the elastic volume change:

$$F_e=dV/dt=(1/\epsilon)\ dP_2/dt. \tag{A4}$$

If air bubbles are present anywhere in the system, they will be compressed according to the ideal gas law as the pressure of the fluid around the bubble increases. If V_b is the volume of a bubble at *absolute* gas pressure, P_b, then the ideal gas law gives:

$$P_bV_b=nRT=P_iV_i \tag{A5}$$

where n is the number of moles of gas in the bubble, R is the gas constant, T is the Kelvin temperature, and P_i and V_i are the initial gas pressure and volume, respectively. If we write

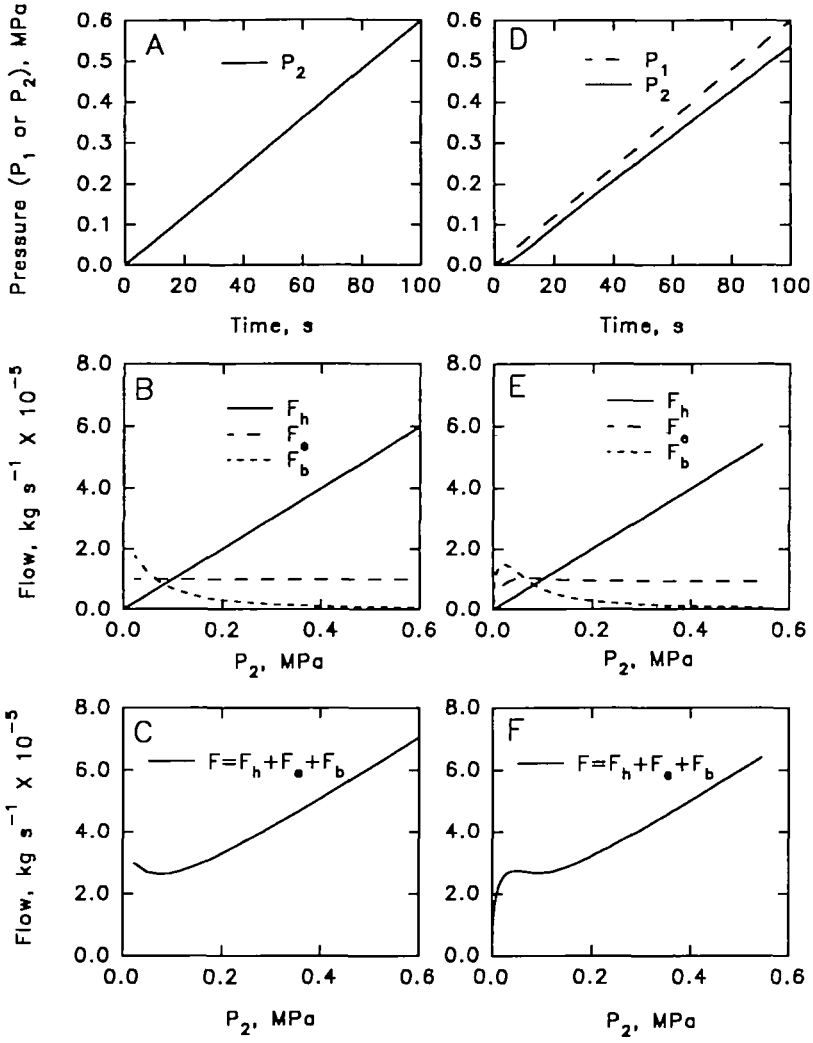

Fig. 9. Theoretical predictions of total flow, F, and its components F_b (Equation A2), F_e (Equation A4), and F_b (Equation A7). (B) and (C) show the flows if P_2 increases linearly with time from time 0 (A). (E) and (F) show the component and total flows if P_1 increases linearly with time causing a short lag in P_2 before it too increases linearly with time. The curves were computed with the following parameters: $K = 1 \times 10^{-4}$ kg s^{-1} MPa^{-1}, $K_{CT} = 1 \times 10^{-3}$ kg s^{-1} MPa^{-1}, $V_iP_i = 4.5 \times 10^{-5}$ m^3 MPa, $\epsilon = 588$ MPa m^{-3}, and a rate of pressure increase = 6 kPa s^{-1}. Compare these theoretical curves to the experimental curves in Figs 3, 4 and 6.

Equation (5a) as $V_b = V_iP_i/P_b$ and take the derivative with time we get the rate of volume change of the bubble:

$$dV_b/dt = -(V_iP_i/P_b^2)dP_b/dt. \quad \text{(A6)}$$

The negative sign of the derivative indicates that V_b decreases with increasing P_b. The flow of water to compress the gas volume is the negative of Equation (A6) so we have:

$$F_b = -dV_b/dt = (V_iP_i/P_b^2)dP_b/dt. \quad \text{(A7)}$$

In the case where all the air bubbles are near the outlet side of the flowmeter, we can equate P_b to $P_2 + P_i$ where P_i is the initial absolute pressure of the bubble when $P_2 = 0$. P_i approximately equals 0.1 MPa and will be determined by the barometric pressure plus the contribution of surface tension of the air–water interface to bubble compression. In the special case where the air bubbles are near the outlet of the flowmeter, the dynamic flow will be given by substituting Equations (A2, A4 and A7) into (A1):

$$F = KP_2 + (1/\epsilon)dP_2/dt + V_iP_i/(P_2 + 0.1)^2 dP_2/dt. \quad \text{(A8)}$$

In our experiments the inlet pressure P_1 increased linearly with time, and after a short time delay this caused P_2 to increase linearly with time which made dP_2/dt equal to a constant. This permitted easier interpretation of results because it made the elastic contribution add as a constant offset to F_h. The contribution of the three terms in Equation (A8) is illustrated in Fig. 9 for the case where P_2 increases linearly with time from time = 0 (Fig. 9A). The component flows (F_h, F_e, and F_b) are shown in Fig. 9B and the total flow is shown in Fig. 9C.

It is not possible, in practice, to make P_2 increase linearly with time from time 0, because an extra conductance equal to the conductance of the capillary tubes of the HPFM (K_{CT}) is interposed between the pressure transducers that measure P_1 and P_2 (Fig. 1). When the full set of equations is derived (not shown) a short time lag is predicted before P_2 increases linearly with time (Fig. 9D). The resulting component and total flows are shown in Fig. 9E and F, respectively.

Air bubbles generally can be avoided within the flowmeter tubing and apparatus, but sometimes air is in the vessels and/or intercellular air spaces in the base of roots. Although the

compression of air bubbles cause an increase in F at any given P_2 during a transient measurement, bubbles cause an underestimation of K_r, because F_b decreases with increasing P_2 causing a negative contribution to the slope used to calculate K_r. Fortunately, the contribution of bubble compression to total flow diminishes with increasing pressure and the slope of the F versus P_2 for $P_2 > 0.25$ MPa is a reasonable approximation of the hydraulic conductance of the root system being measured. It is probably good practice to measure transient flows for P_2 up to 0.5 MPa in order to reduce the underestimation of K_r caused by compression of air bubbles.

References

Caldwell MM. 1976. Root extension and water absorption. In: Lange OL, Kappen L, Schulze E-D, eds. *Water and plant life*. Berlin and New York: Springer-Verlag, 63–85.

Dawson TE. 1993. Hydraulic lift and water use by plants: implications for water balance, performance and plant–plant interactions. *Oecologia* **95,** 565–74.

Levy Y, Syvertsen JP, Nemec S. 1983. Effect of drought stress and vesicular arbuscular mycorrhiza on citrus transpiration and hydraulic conductivity of roots. *New Phytologist* **93,** 61–6.

Markhart AH, Smit B. 1990. Measurement of root hydraulic conductance. *Horticultural Science* **25,** 282–7.

Melchior W, Steudle E. 1993. Water transport in onion (*Allium cepa* L.) roots. *Plant Physiology* **101,** 1305–15.

Newman EI. 1969. Resistance to water flow in soil and plant. I. Soil resistance in relation to amounts of root: Theoretical estimates. *Journal of Applied Ecology* **6,** 1–12.

Nobel PS, Sanderson J. 1984. Rectifier-like activities of roots of two desert succulents. *Journal of Experimental Botany* **35,** 727–37.

Ramos C, Kaufmann MR. 1979. Hydraulic resistance of rough lemon roots. *Physiologia Plantarum* **45,** 311–14.

Richards JH, Caldwell MM. 1987. Hydraulic lift: Substantial nocturnal water transport between soil layers by *Artemisia tridentata* roots. *Oecologia* **73,** 486–9.

Saliendra NZ, Meinzer FC. 1992. Genotypic, developmental and drought-induced differences in root hydraulic conductance of contrasting sugarcane cultivars. *Journal of Experimental Botany* **43,** 1209–17.

Salim M, Pitman MG. 1984. Pressure-induced water and solute flow through plant roots. *Journal of Experimental Botany* **35,** 869–81.

Steudle E. 1993. Pressure probe techniques: basic principles and application to studies of water and solute relations at the cell, tissue and organ level. In: Smith JAC, Griffiths H, eds. *Water deficits: plant responses from cell to community*. Oxford, UK: BIOS Scientific Publishers Ltd, 5–36.

Tyree MT. 1983. Maple sap uptake, exudation, and pressure changes correlated with freezing exotherms and thawing endotherms. *Plant Physiology* **73,** 277–85.

Tyree MT, Ewers FW. 1991. The hydraulic architecture of trees and other woody plants. *New Phytologist* **19,** 345–60.

Tyree MT, Yang S, Cruiziat P, Sinclair B. 1994. Novel methods of measuring hydraulic conductivity of tree root systems and interpretation using AMAIZED: A maize-root dynamic model for water and solute transport. *Plant Physiology* **104,** 189–99.

Yang S, Tyree MT. 1994. Hydraulic architecture of *Acer saccharum* and *A. rubrum* comparison of branches to whole trees and the contribution of leaves to hydraulic resistance. *Journal of Experimental Botany* **45,** 179–86.